Topics in time-frequency analysis

Maria Sandsten

Lecture 7
Stationary and non-stationary spectral analysis

February 10 2020

Wigner distribution

The **Wigner distribution** is defined as,

$$W_z(t,f) = \int_{-\infty}^{\infty} z(t+\frac{\tau}{2}) z^*(t-\frac{\tau}{2}) e^{-i2\pi f\tau} d\tau,$$

with t is time, f is frequency and $z(t)$ is the analytic signal. The **ambiguity function** is defined as

$$A_z(\nu,\tau) = \int_{-\infty}^{\infty} z(t+\frac{\tau}{2}) z^*(t-\frac{\tau}{2}) e^{-i2\pi \nu t} dt,$$

where ν is the **doppler frequency** and τ is the **lag variable**.

Ambiguity function

Facts about the ambiguity function:

- The auto-terms are always centered at $\nu = \tau = 0$.
- The phase of the ambiguity function oscillations are related to centre t_0 and f_0 of the signal.
- $|A_{z_1}(\nu, \tau)| = |A_{z_0}(\nu, \tau)|$ when $W_{z_1}(t, f) = W_{z_0}(t - t_0, f - f_0)$.
- The cross-terms are always located away from the centre.
- The placement of the cross-terms are related to the interconnection of the auto-terms.

The quadratic class

The quadratic or Cohen's class is usually defined as

$$W_z^Q(t,f) = \int_{-\infty}^{\infty}\int_{-\infty}^{\infty}\int_{-\infty}^{\infty} z(u+\frac{\tau}{2})z^*(u-\frac{\tau}{2})\phi(\nu,\tau)e^{i2\pi(\nu t - f\tau - \nu u)}\,du\,d\tau\,d\nu.$$

The filtered ambiguity function can also be formulated as

$$A_z^Q(\nu,\tau) = A_z(\nu,\tau)\cdot\phi(\nu,\tau),$$

and the corresponding smoothed Wigner distribution as

$$W_z^Q(t,f) = W_z(t,f) * *\Phi(t,f),$$

using the corresponding time-frequency kernel.

Properties of the ambiguity kernel

In order to preserve the marginals and the total energy condition of the time-frequency distribution, the ambiguity kernel must fulfill

$$\phi(0,\tau) = \phi(\nu,0) = 1, \quad \phi(0,0) = 1.$$

For a real-valued distribution,

$$\phi^*(-\nu,-\tau) = \phi(\nu,\tau).$$

The Choi-Williams distribution

The Choi-Williams distribution or the Exponential distribution (ED), is defined from the ambiguity kernel

$$\phi_{ED}(\nu,\tau) = e^{-\frac{\nu^2\tau^2}{\sigma}},$$

where σ is a design parameter. The distribution satisfies the marginals and total energy condition,

$$\phi_{ED}(0,\tau) = \phi_{ED}(\nu,0) = 1, \quad \phi_{ED}(0,0) = 1.$$

The Choi-Williams distribution is real-valued,

$$\phi^*_{ED}(-\nu,-\tau) = e^{-\frac{\nu^2\tau^2}{\sigma}} = \phi_{ED}(\nu,\tau).$$

The Choi-Williams distribution works well for suppression of cross-terms found on a diagonal line between the auto-terms.

Example

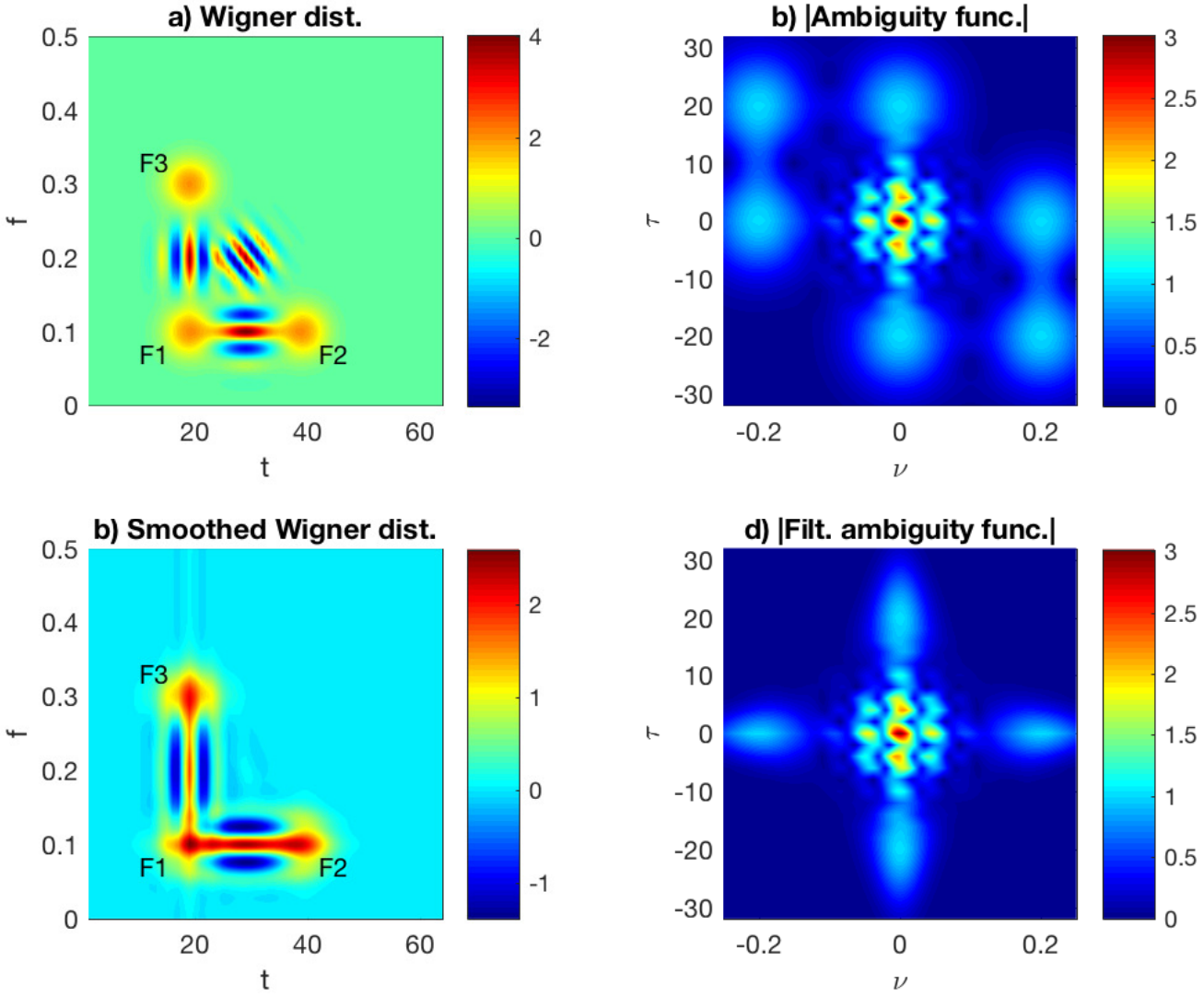
a) Wigner dist.
F3
F1
F2
f
t
b) |Ambiguity func.|
τ
ν
b) Smoothed Wigner dist.
F3
F1
F2
f
t
d) |Filt. ambiguity func.|
τ
ν

Separable kernels

Separable kernels is defined by

$$\phi(\nu, \tau) = G_1(\nu) \cdot g_2(\tau),$$

The smoothed Wigner-Ville distribution becomes

$$W_z^F(t, f) = W_z(t, f) * *\Phi(t, f) = g_1(t) * W_z(t, f) * G_2(f).$$

- If $G_1(\nu) = 1$ a **doppler-independent** kernel is given as $\phi(\nu, \tau) = g_2(\tau)$, resulting in the **pseudo-Wigner distribution**, with smoothing only in frequency.
- If $g_2(\tau) = 1$ a **lag-independent** kernel is $\phi(\nu, \tau) = G_1(\nu)$ where the time-frequency formulation gives smoothing only in time.

Doppler-independent kernel

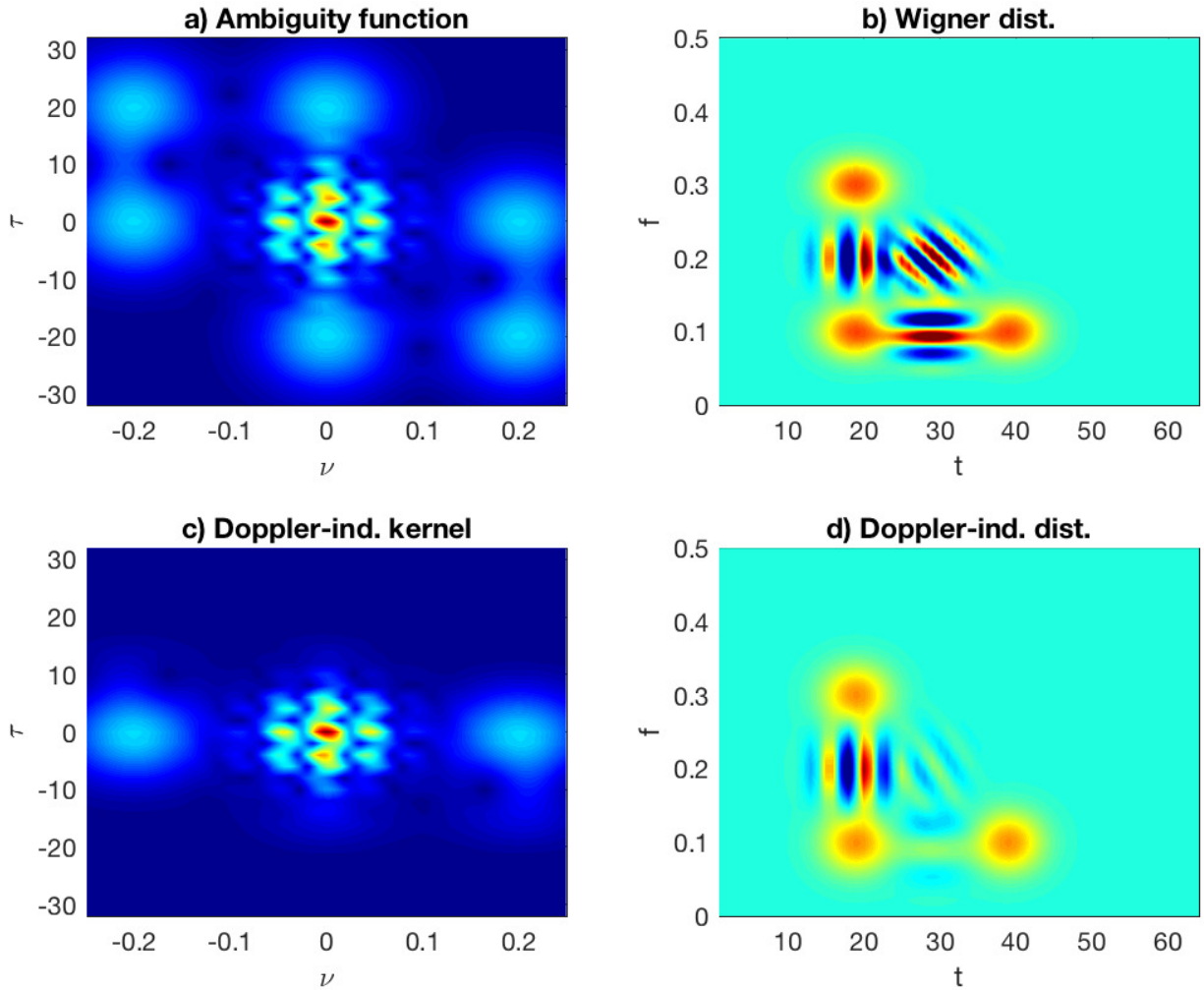

Lag-independent kernel

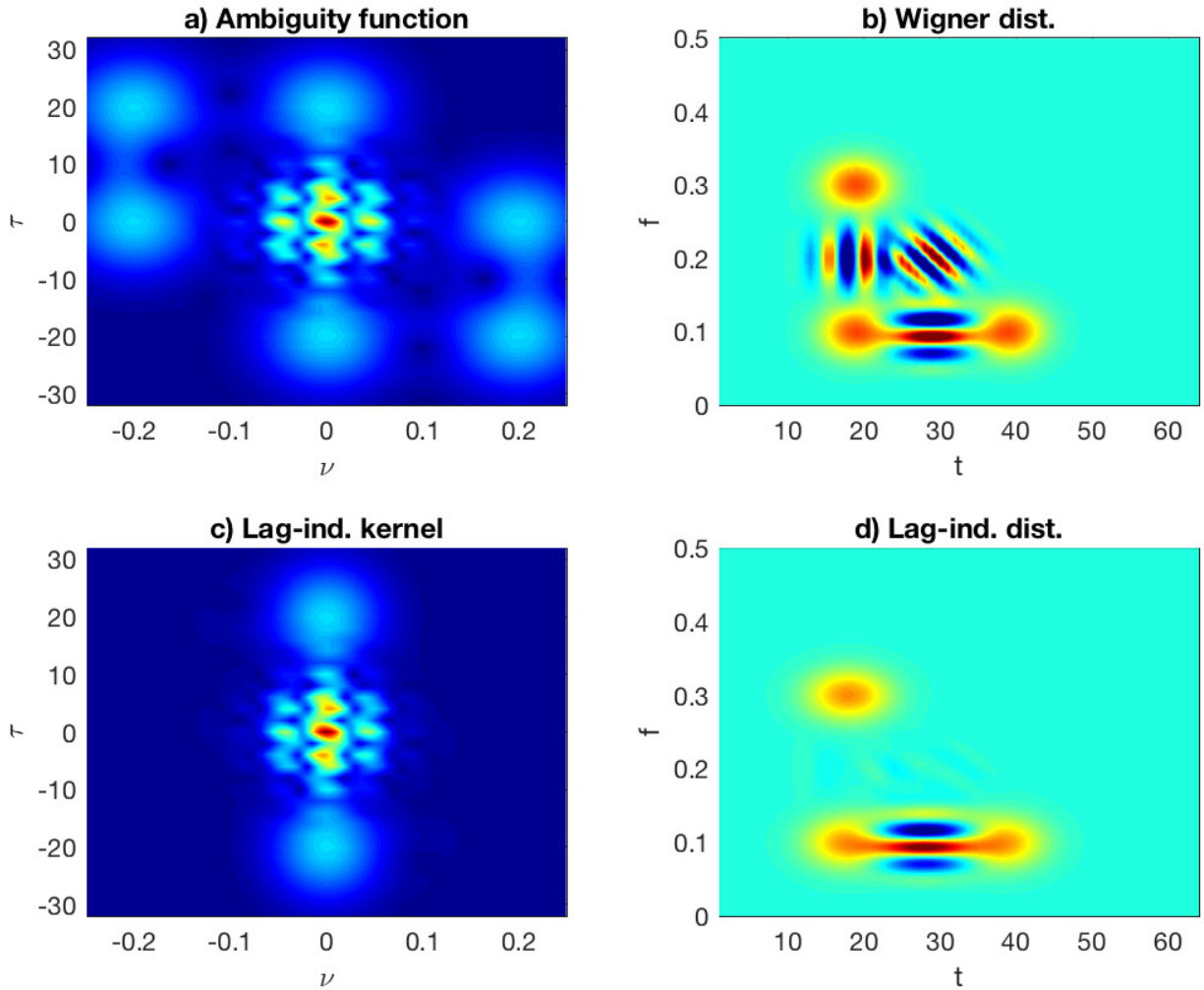

The Rihaczek distribution

The energy of a complex-valued signal is

$$\begin{aligned} E &= \int_{-\infty}^{\infty} |z(t)|^2 dt = \int_{-\infty}^{\infty} z(t) z^*(t) dt \\ &= \int_{-\infty}^{\infty} \int_{-\infty}^{\infty} z(t) Z^*(f) e^{-i2\pi ft} df dt. \end{aligned}$$

The **Rihaczek distribution** is defined as

$$R_z(t, f) = z(t) Z^*(f) e^{-i2\pi ft}.$$

The Rihaczek distribution

The marginals are satisfied as

$$\int_{-\infty}^{\infty} R_z(t,f)df = z(t)\int_{-\infty}^{\infty} Z^*(f)e^{-i2\pi ft}df = |z(t)|^2,$$

and

$$\int_{-\infty}^{\infty} R_z(t,f)dt = Z^*(f)\int_{-\infty}^{\infty} z(t)e^{-i2\pi ft}dt = |Z(f)|^2.$$

The ambiguity kernel is found as

$$\phi(\nu,\tau) = e^{-i\pi\nu\tau}. \quad (\textit{Assignment}!)$$

From this expression we also easily verify that the marginals are satisfied as $\phi(\nu,0) = \phi(0,\tau) = 1$. Is the Rihaczek distribution real-valued?

$$(\phi^*(-\nu,-\tau) = \phi(\nu,\tau)?).$$

Example

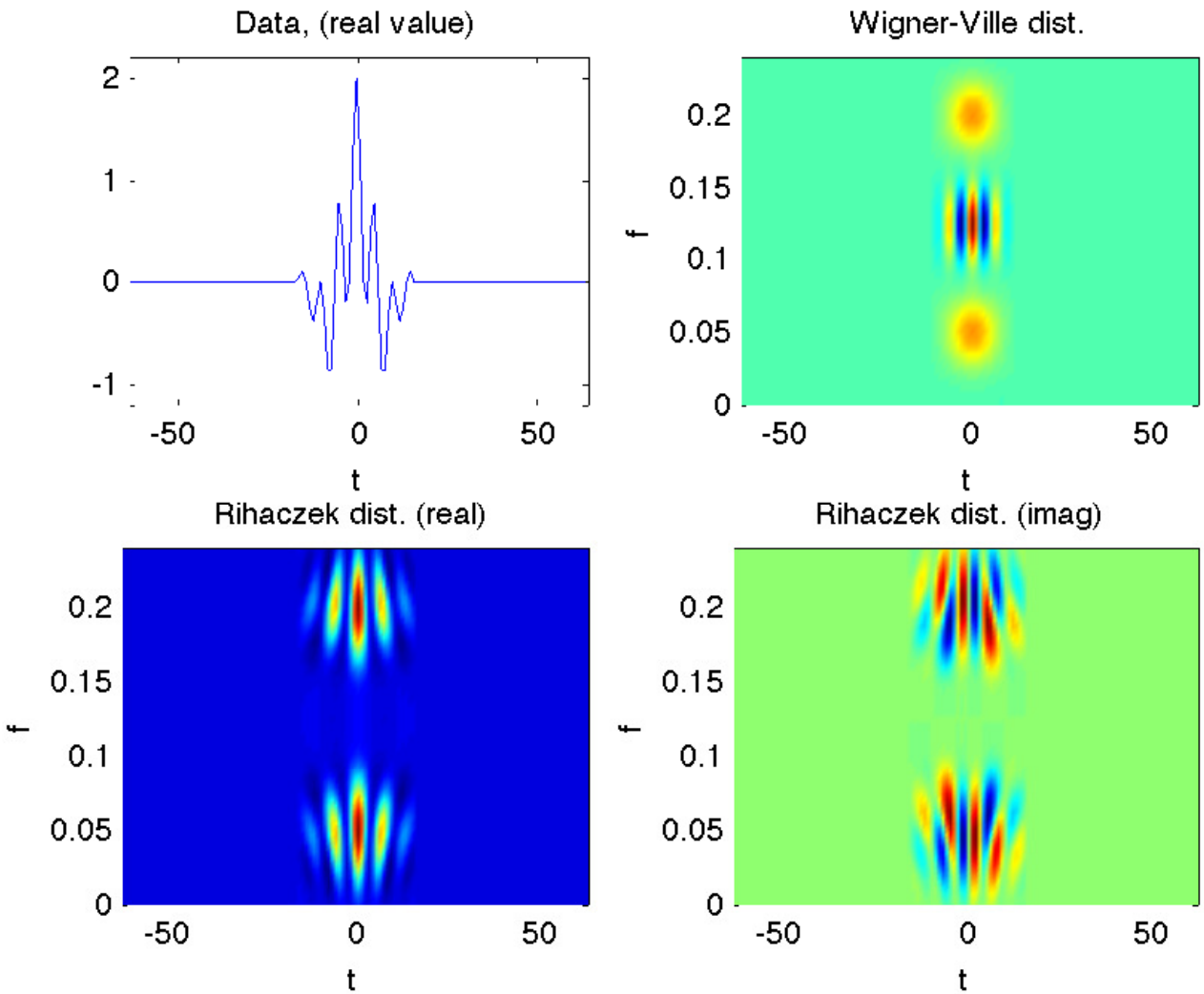
Data, (real value)
2
1
0
-1
-50
0
50
t
Wigner-Ville dist.
0.2
0.15
0.1
0.05
0
f
-50
0
50
t
Rihaczek dist. (real)
0.2
0.15
0.1
0.05
0
f
-50
0
50
t
Rihaczek dist. (imag)
0.2
0.15
0.1
0.05
0
f
-50
0
50
t

Example

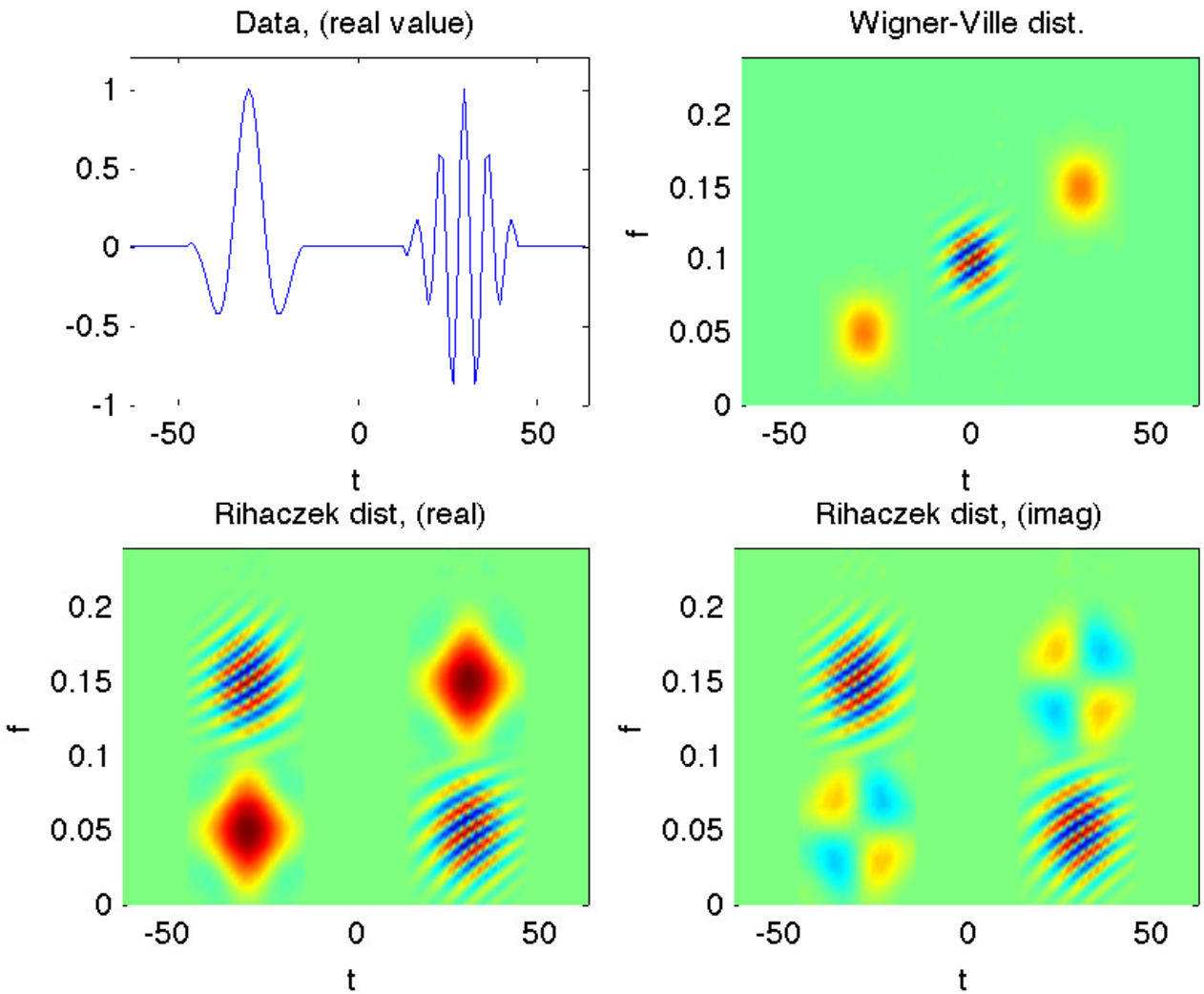
Data, (real value)
1
0.5
0
-0.5
-1
-50
0
50
t
Wigner-Ville dist.
0.2
0.15
0.1
0.05
0
f
-50
0
50
t
Rihaczek dist, (real)
0.2
0.15
0.1
0.05
0
f
-50
0
50
t
Rihaczek dist, (imag)
0.2
0.15
0.1
0.05
0
f
-50
0
50
t

The spectrogram again

We can also formulate the quadratic class as

$$W_z^Q(t,f) = \int_{-\infty}^{\infty}\int_{-\infty}^{\infty} r_z(u,\tau)\rho(t-u,\tau)e^{-i2\pi f\tau}\,du\,d\tau,$$

where the **time-lag kernel** is defined as

$$\rho(t,\tau) = \int_{-\infty}^{\infty} \phi(\nu,\tau)e^{i2\pi\nu t}\,d\nu,$$

and the IAF as

$$r_z(t,\tau) = z(t+\frac{\tau}{2})z^*(t-\frac{\tau}{2}).$$

(Assignment!)

The spectrogram kernel

The spectrogram also belongs to the quadratic class which can be seen from the following derivation:

$$S_z(t,f) = |\int_{-\infty}^{\infty} h^*(t_1 - t)z(t_1)e^{-i2\pi f t_1}\,dt_1|^2,$$

$$= (\int_{-\infty}^{\infty} h^*(t_1 - t)z(t_1)e^{-i2\pi f t_1}\,dt_1)(\int_{-\infty}^{\infty} h(t_2 - t)z^*(t_2)e^{i2\pi f t_2}\,dt_2).$$

With $t_1 = u + \frac{\tau}{2}$ and $t_2 = u - \frac{\tau}{2}$, we get $S_z(t,f) =$

$$= \int_{-\infty}^{\infty}\int_{-\infty}^{\infty} z(u+\frac{\tau}{2})z^*(u-\frac{\tau}{2})h^*(u+\frac{\tau}{2}-t)h(u-\frac{\tau}{2}-t)e^{-i2\pi f\tau}\,d\tau\,du.$$

The spectrogram kernel

We can identify the time-lag distribution

$$r_z(u,\tau) = z(u+\frac{\tau}{2})z^*(u-\frac{\tau}{2}),$$

and the time-lag kernel

$$\rho_h(t-u,\tau) = h^*(u-t+\frac{\tau}{2})h(u-t-\frac{\tau}{2}),$$

giving

$$S_z(t,f) = \int_{-\infty}^{\infty}\int_{-\infty}^{\infty} r_z(u,\tau)\rho_h(t-u,\tau)e^{-i2\pi f\tau}d\tau du,$$

which we recognize as the quadratic class.

The spectrogram kernel

The window function can be expressed as an ambiguity kernel $\phi_h(\nu, \tau)$ which is the ambiguity function of a window $h(t)$, i.e.,

$$\phi_h(\nu, \tau) = \int_{-\infty}^{\infty} h^*(-t + \frac{\tau}{2}) h(-t - \frac{\tau}{2}) e^{-i2\pi\nu t} dt.$$

The spectrogram does not fulfill the marginals. Why?

Example

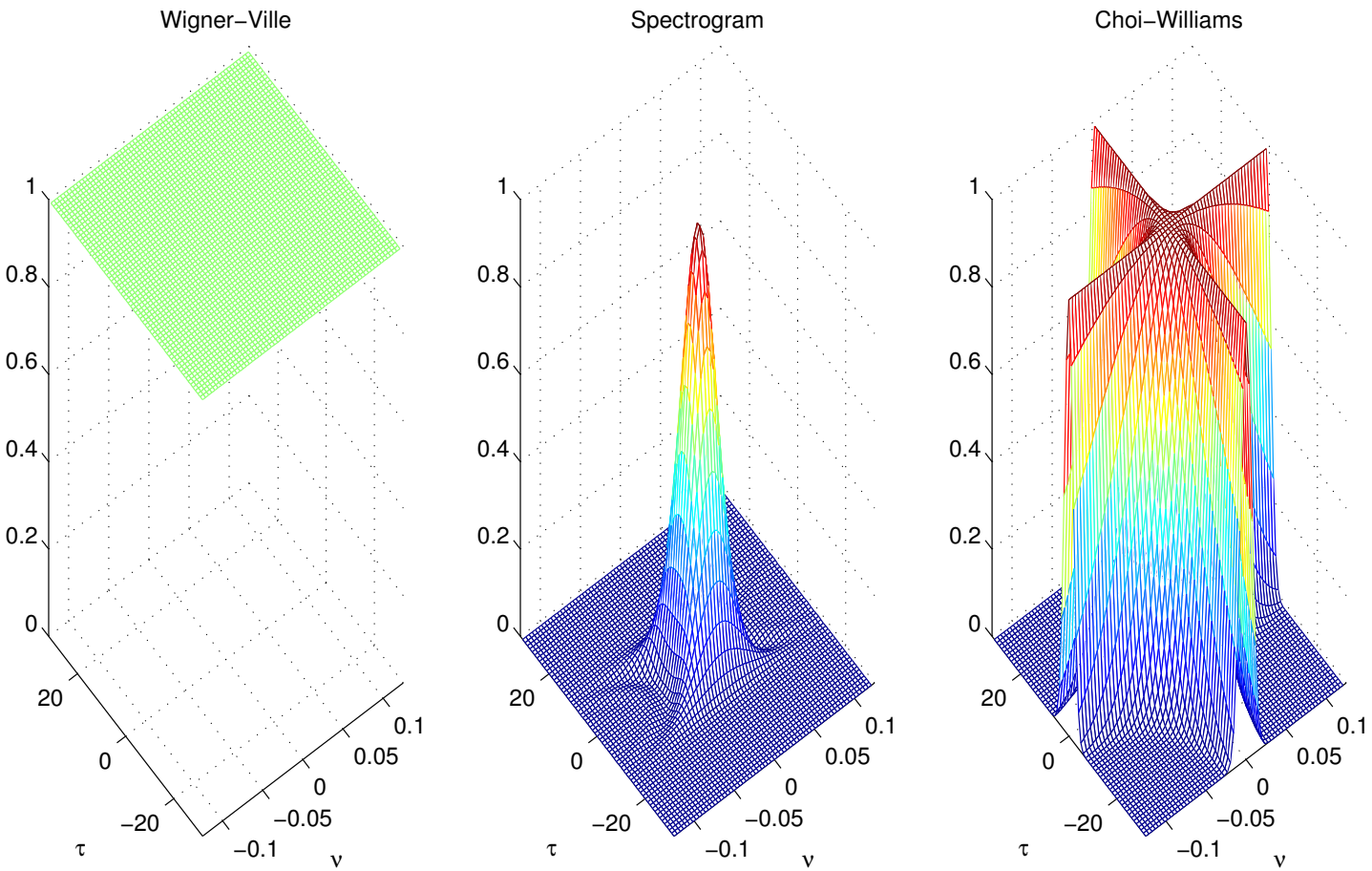
Wigner–Ville
Spectrogram
Choi–Williams
1
0.8
0.6
0.4
0.2
0
20
0
−20
τ
0.1
0.05
0
−0.05
−0.1
ν

Multitaper spectrogram analysis

Replacement with $u = (t_1 + t_2)/2$ and $\tau = t_1 - t_2$ in

$$W_z^Q(t,f) = \int_{-\infty}^{\infty}\int_{-\infty}^{\infty} r_z(u,\tau)\rho(t-u,\tau)e^{-i2\pi f\tau}\,du\,d\tau,$$

give

$$W_z^Q(t,f) = \int\int r_z(\frac{t_1+t_2}{2}, t_1-t_2)\rho(t-\frac{t_1+t_2}{2}, t_1-t_2)e^{-i2\pi f(t_1-t_2)}dt_1 dt_2,$$

where the IAF

$$r_z(\frac{t_1+t_2}{2}, t_1-t_2) = z(\frac{t_1+t_2}{2}+\frac{t_1-t_2}{2})z^*(\frac{t_1+t_2}{2}-\frac{t_1-t_2}{2}) = z(t_1)z^*(t_2).$$

Multitaper spectrogram analysis

Define a **rotated time-lag kernel** as

$$\rho^{rot}(t_1, t_2) = \rho(\frac{t_1 + t_2}{2}, t_1 - t_2),$$

and we get

$$W_z^Q(t, f) = \int \int z(t_1) z^*(t_2) \rho^{rot}(t - t_1, t_2) e^{-i2\pi f t_1} e^{i2\pi f t_2} dt_1 dt_2.$$

If the kernel $\rho^{rot}(t_1, t_2) = (\rho^{rot}(t_2, t_1))^*$, then solving the integral

$$\int \rho^{rot}(t_1, t_2) u(t_1) dt_1 = \lambda \; u(t_2),$$

results in eigenvalues λ_k and eigenfunctions $u_k(t)$.

Multitaper spectrogram analysis

The quadratic class for any kernel is now rewritten as a weighted sum of spectrograms,

$$W_z^Q(t,f) = \sum_{k=1}^{\infty} \lambda_k \left| \int z(t_1) e^{-i2\pi f t_1} u_k^*(t-t_1) dt_1 \right|^2.$$

The quadratic class of time-frequency distributions can always be approximated,

$$W_z^Q(t,f) \approx \sum_{k=1}^{K} \lambda_k \left| \int z(t_1) e^{-i2\pi f t_1} u_k^*(t-t_1) dt_1 \right|^2,$$

where K is chosen as the number including all $\lambda_k > \epsilon$. If K is reasonable small, the computations are efficient.

Classification of time-frequency representations

$$S_z(t,f) = \Phi^h(t,f) ** W_z(t,f) \approx \sum_{j=1}^{M} s_j \cdot \mathbf{u}_j(t) * \left(\mathbf{v}_j(f)^T * W_z(t,f) \right),$$

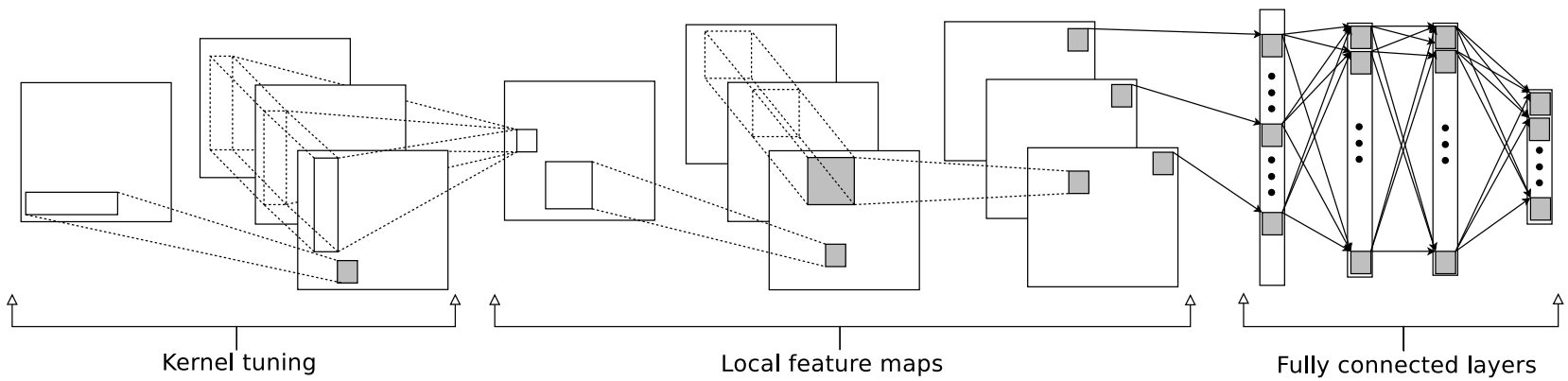

Johan Brynolfsson and Maria Sandsten, "Classification of One-Dimensional Non-Stationary Signals Using the Wigner-Ville Distribution in Convolutional Neural Networks, EUSIPCO, Kos island, Greece, 2017.

Classification of time-frequency representations

Eight different classes of multi-component chirp signals (class 1 and 2), sinusoids (class 3-6) and multi-component short Gaussian signals (class 7 and 8). Stochastic variation in amplitudes, time locations and frequencies.

2017 25th European Signal Processing Conference (EUSIPCO)

True class \ Predicted class	1	2	3	4	5	6	7	8
1	96	4	-	-	-	-	-	-
2	7	93	-	-	-	-	-	-
3	-	-	100	-	-	-	-	-
4	-	-	6	94	-	-	-	-
5	-	-	-	-	86	14	-	-
6	-	-	-	-	1	99	-	-
7	-	-	-	-	-	-	74	26
8	-	-	-	-	-	-	2	98

Table III: Confusion matrix for WVD-ktCNN rounded to nearest integer percent.

True class \ Predicted class	1	2	3	4	5	6	7	8
1	89	10	-	-	-	-	-	-
2	20	80	-	-	-	-	-	-
3	-	-	99	1	-	-	-	-
4	-	-	3	97	-	-	-	-
5	-	-	-	-	88	12	-	-
6	-	-	-	-	6	94	-	-
7	-	-	-	-	-	-	49	51
8	-	-	-	-	-	-	28	71

Table IV: Confusion matrix for spect-CNN rounded to nearest integer percent.

The Thomson multitapers

Maximize the energy from the FIR-filter with frequency function $H(f) = \mathbf{h}^T \mathbf{W}(f)$ and use a predefined bandwidth B, i.e.

$$\begin{aligned} P_B &= \int_{-B/2}^{B/2} |H(f)|^2 S_x(f) df = \mathbf{h}^T \int_{-B/2}^{B/2} \Phi(f) S_x(f) \Phi^*(f) df \mathbf{h} \\ &= \mathbf{h}^T \int_{-\infty}^{\infty} \Phi(f) S_B(f) \Phi^*(f) df \mathbf{h} = \mathbf{h}^T \mathbf{R}_B \mathbf{h}, \end{aligned}$$

with constrained filter energy as

$$\int_{-1/2}^{1/2} |H(f)|^2 df = \mathbf{h}^T \mathbf{h} = 1.$$

The initial expression has similarities with the Capon algorithm, but it is NOT the same optimization!

The Thomson multitaper method

The solution of the eigenvalue problem

$$\mathbf{R}_B\mathbf{h} = \lambda\mathbf{h},$$

will give the maximum energy as

$$P_B = \mathbf{h}^T\mathbf{R}_B\mathbf{h} = \lambda\mathbf{h}^T\mathbf{h} = \lambda,$$

i.e. λ gives the percentage of energy inside the frequency band B. The eigenvectors are orthogonal so with the choice of K possible eigenvectors, which all correspond to largest eigenvalues, λ_k, we have a set of orthonormal windows, multitapers, $\mathbf{h}_k$, which maximize the filter energy. The multitaper spectrum is calculated as

$$S(f) = \frac{1}{K}\sum_{k=1}^{K} \mid \sum_{t=0}^{n-1} x(t)h_k(t)e^{-i2\pi ft} \mid^2 .$$

The Thomson multitapers

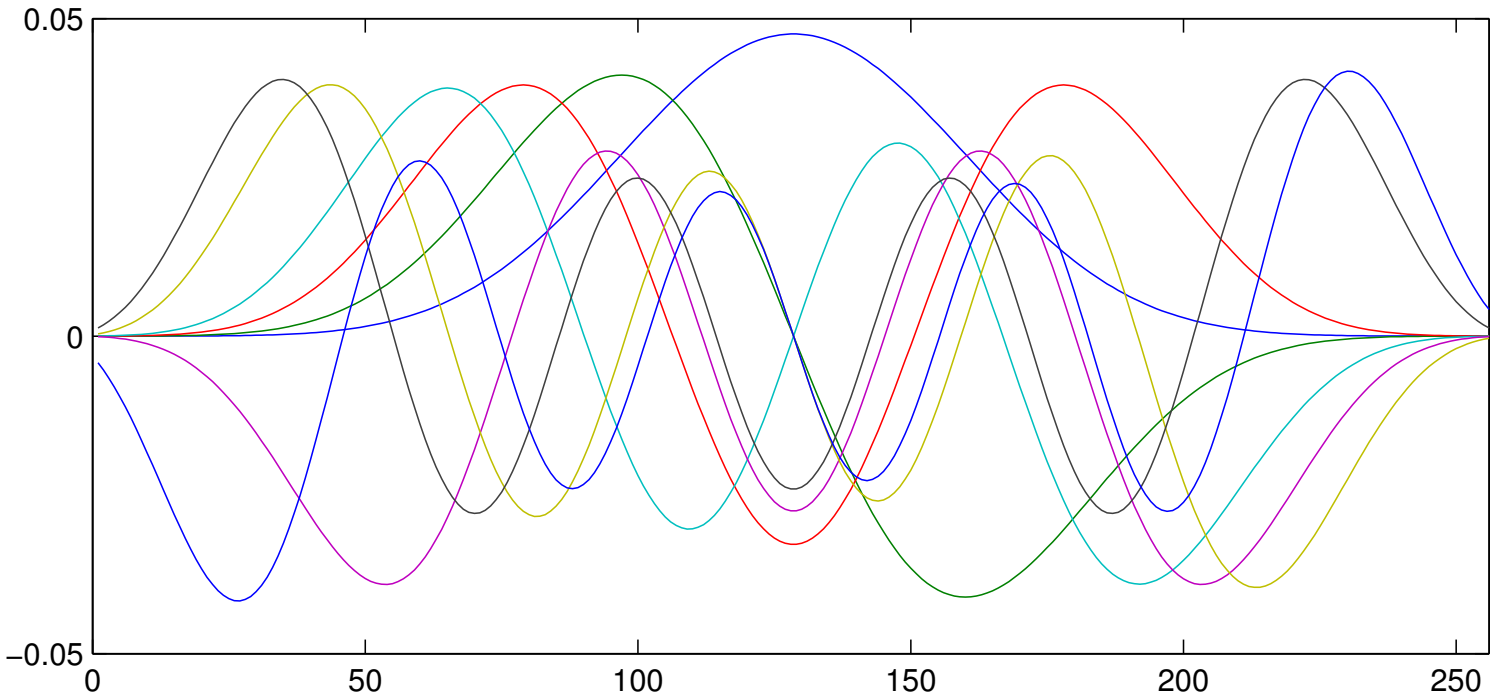

David Thomson, 'Spectrum Estimation and Harmonic Analysis', Proceedings of the IEEE, 1982

David Slepian, 'Prolate Spheroidal Wave Functions, Fourier Analysis, and Uncertainty - V: The Discrete Case', The Bell System Technical Journal, 1978.

The first Thomson multitaper, the Slepian window

A comparison of the window spectrum of the Slepian window, also defined as the first discrete prolate spheroidal sequence (DPSS) (green line) with the Hanning and rectangular window spectra (red and blue lines).

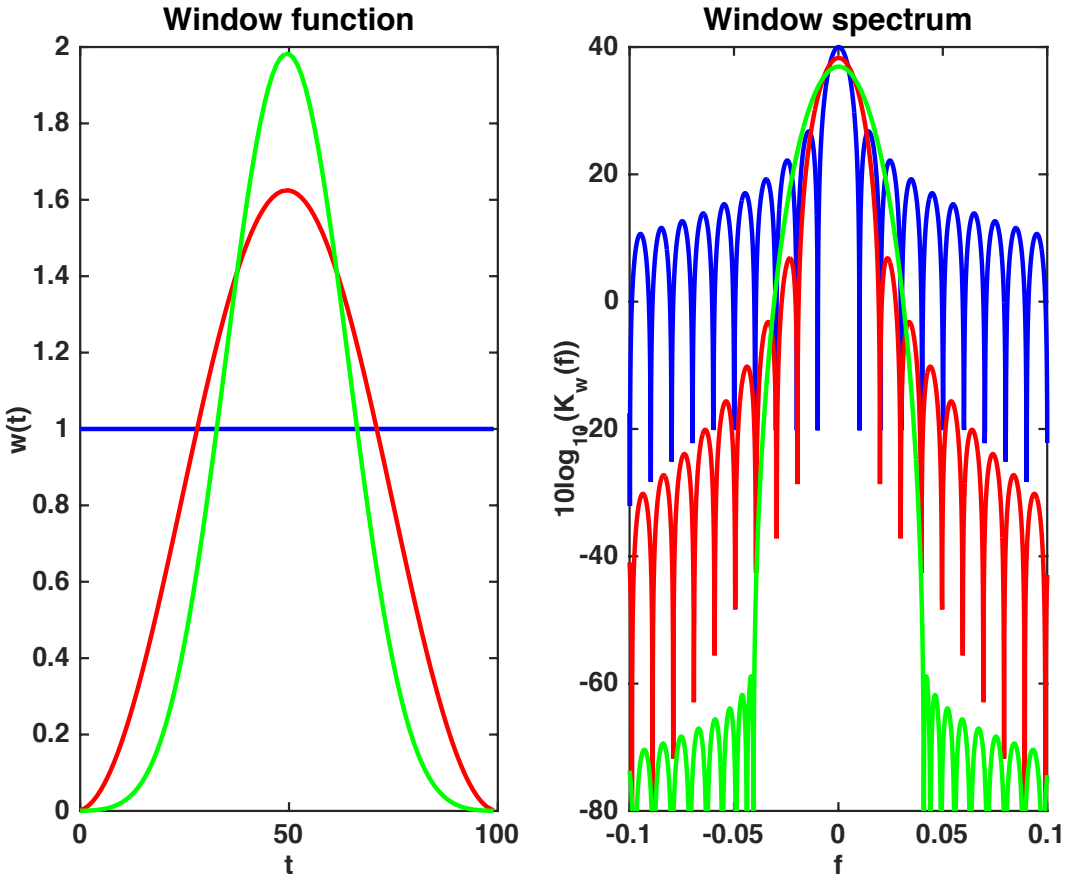

Example

The Slepian window is the best when the dynamics of the estimate is more important than the resolution.

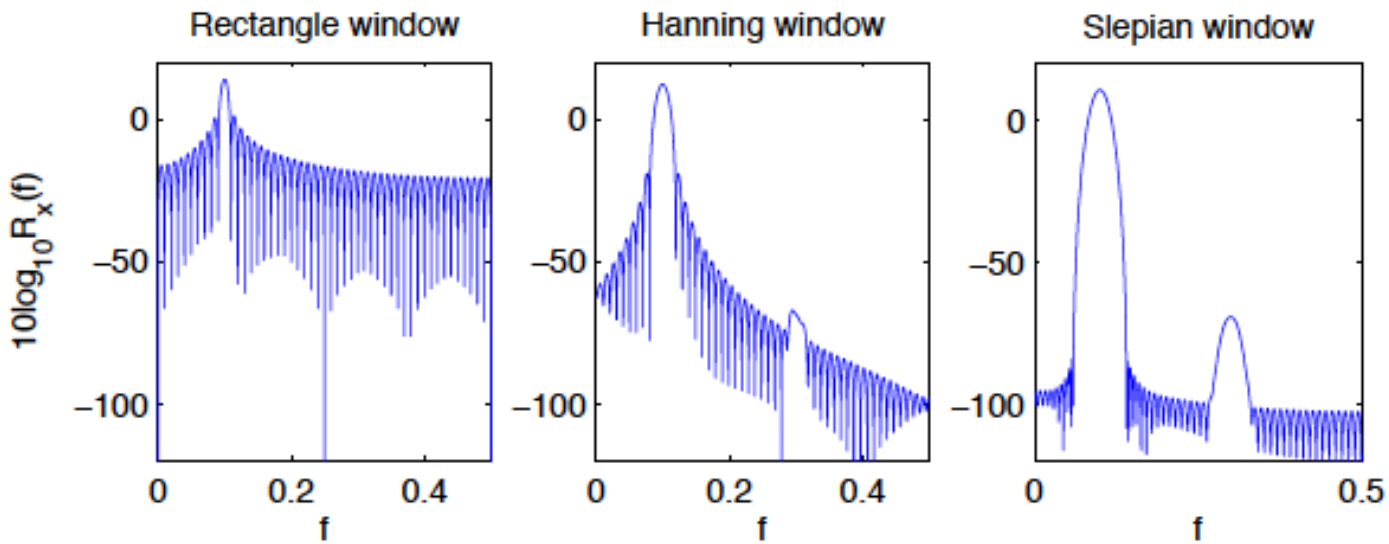

Figure 9.7 *Leakage properties of different windows for two sinusoids with different power using different window functions, $n = 100$.*

A generalized eigenvalue problem

Constrain the total energy even better with use of a penalty function that is large outside the bandwidth B,

$$\int_{-1/2}^{1/2} S_p(f)|H(f)|^2 df = \mathbf{h}^T \mathbf{R}_p \mathbf{h} = 1$$

The solution is given from a generalized eigenvalue problem,

$$\mathbf{R}_B \mathbf{h} = \lambda \mathbf{R}_p \mathbf{h}.$$

Further, it has been shown that a mean square error optimal estimate is given using a weighted multitaper spectrogram, where the weights are represented by the eigenvalues,

$$S(f) = \frac{1}{K} \sum_{k=1}^{K} \alpha_k \mid \sum_{t=0}^{n-1} x(t) h_k(t) e^{-i2\pi ft} \mid^2 .$$

The Peak Matched Multiple Windows

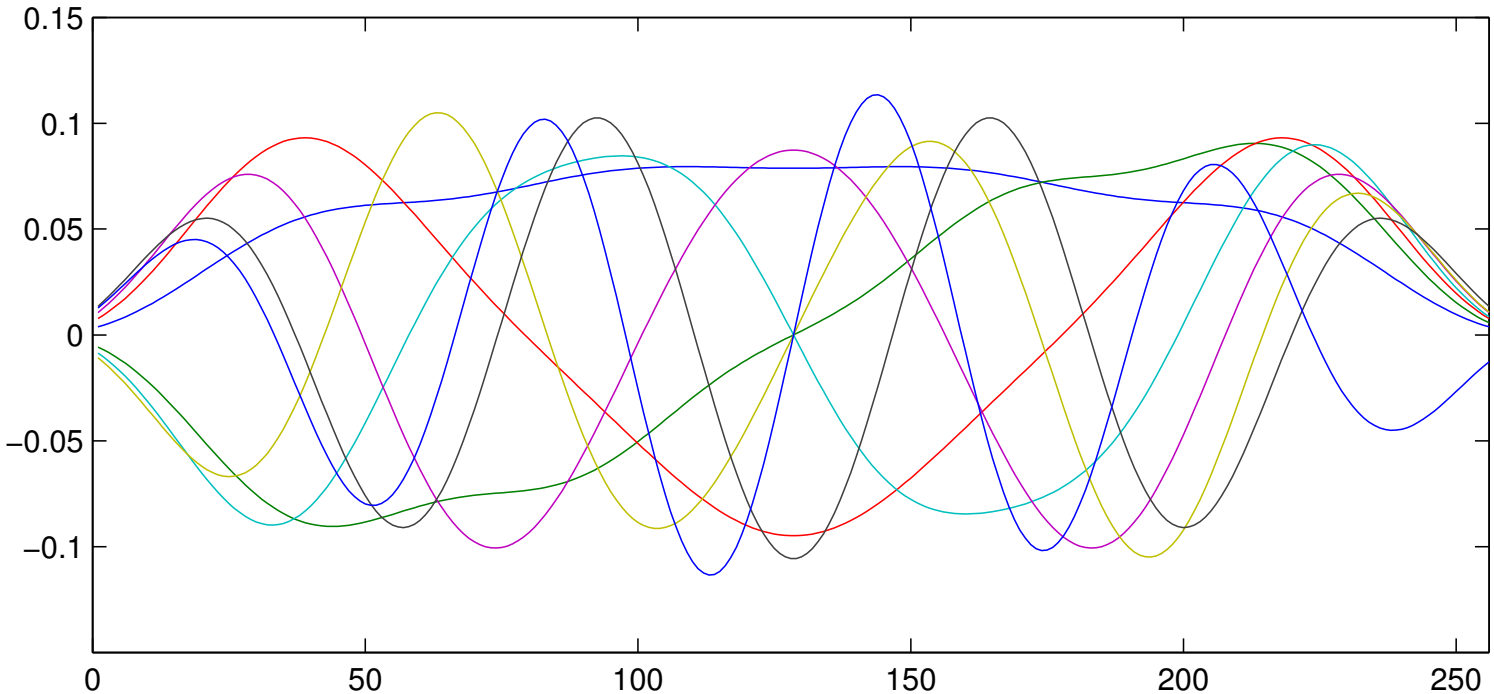

Maria Hansson and Göran Salomonsson, "A Multiple Window Method for Estimation of Peaked Spectra", IEEE Trans. on Signal Processing, Vol. 45, No. 3, March 1997.

Maria Hansson, "Optimized Weighted Averaging of Peak Matched Multiple Window Spectrum Estimates", IEEE Trans. on Signal Processing, Vol. 47, No. 4, April 1999.

Evaluation

The PM MW are shown to have smaller bias as well as variance than the Thomson multitapers, the sinusoidal multitapers and the Welch method for spectrum with sharp peaks.

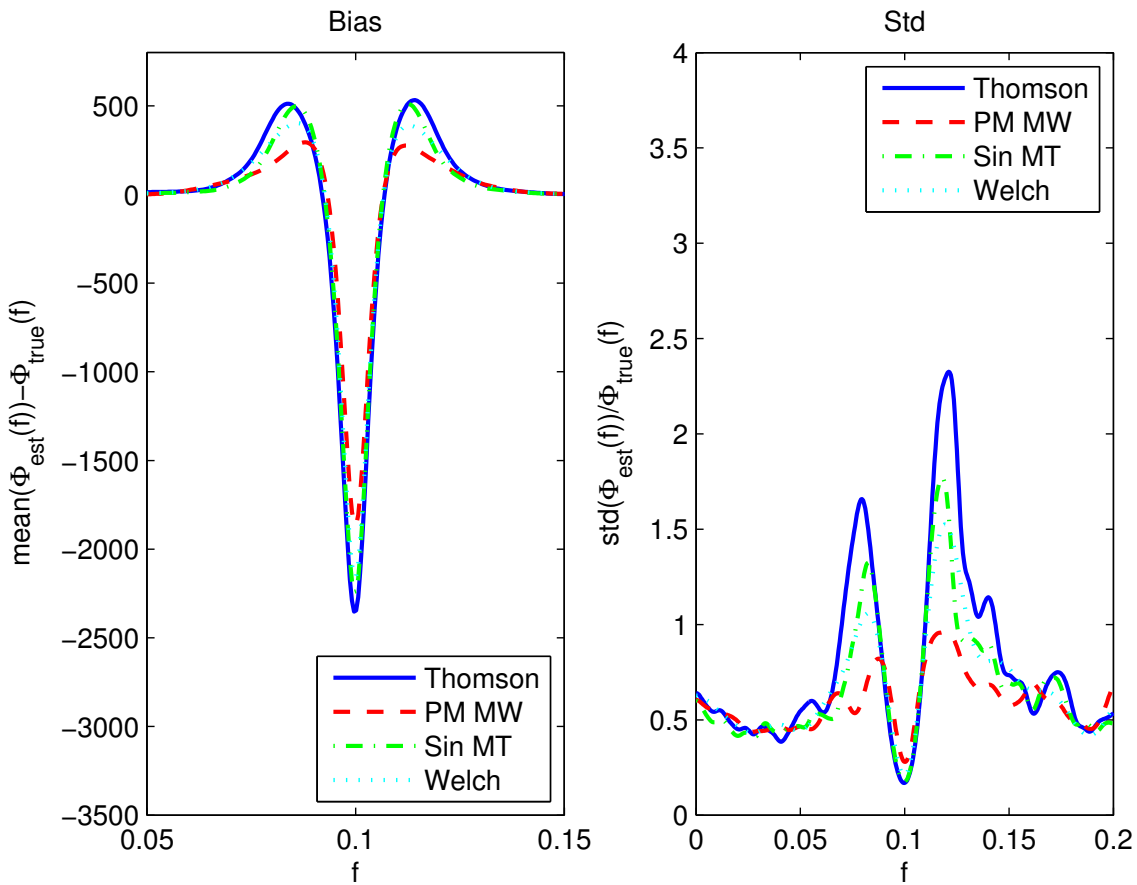

Multitaper spectrogram analysis

A general multitaper spectrogram is defined as

$$S_z(t,f) = \sum_{k=1}^{K} \alpha_k \left| \int_{-\infty}^{\infty} z(t_1) h_k^*(t_1 - t) e^{-i2\pi f t_1} dt_1 \right|^2,$$

where K is the number of multitapers. If K is reasonable small, the computations are efficient. The number of windows K and the weights α_k can be adaptive and optimized to fulfill certain restrictions.

Multitaper spectrogram analysis

In stationary spectral analysis, the **DPSS**s of the Thomson multitapers are well established. The Slepian functions are recognized to give orthonormal spectra, (for stationary white noise) and to be the most localized tapers in the frequency domain. In **time-frequency analysis**, the **Hermite functions** have been shown to give the best time-frequency localization and orthonormality properties.

Ingrid Daubechies, 'Time-Frequency Localization Operators: A Geometric Phase Space Approach', IEEE Trans. on Information Theory, 1988.

Generalized eigenvalue problems

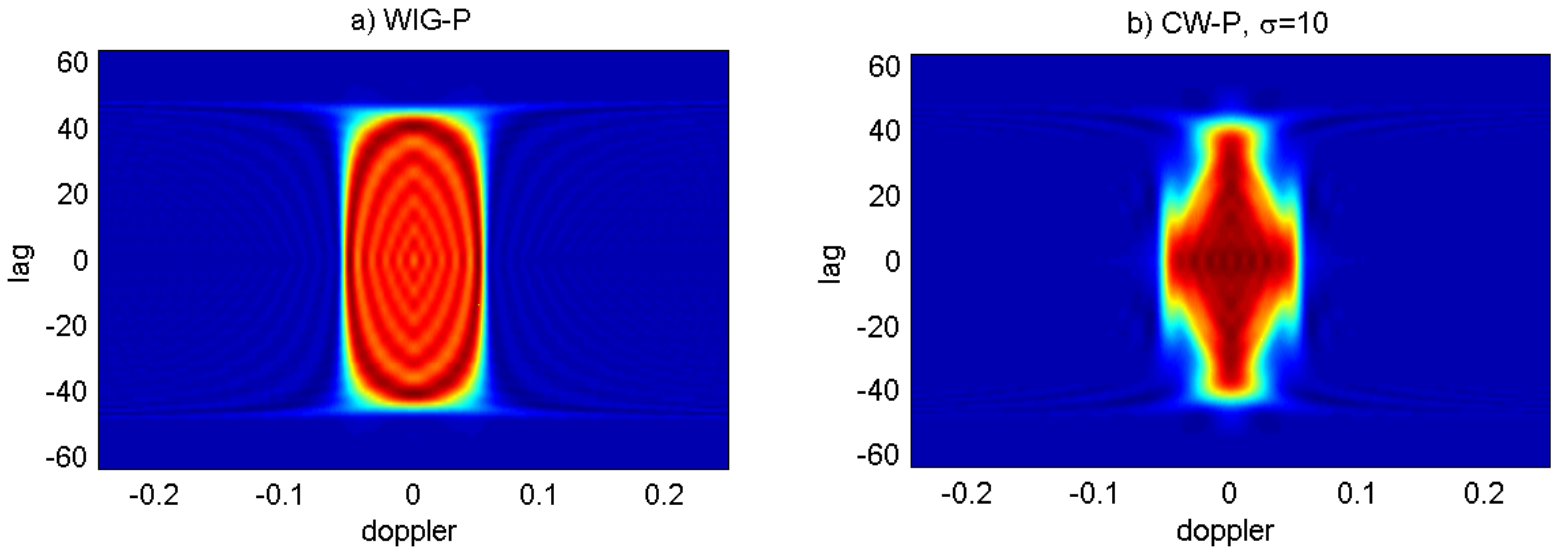

Maria Hansson-Sandsten,'Multitaper Wigner and Choi-Williams distributions with predetermined Doppler-lag bandwidth and sidelobe suppression, Signal Processing, 2011.

Generalized eigenvalue problems

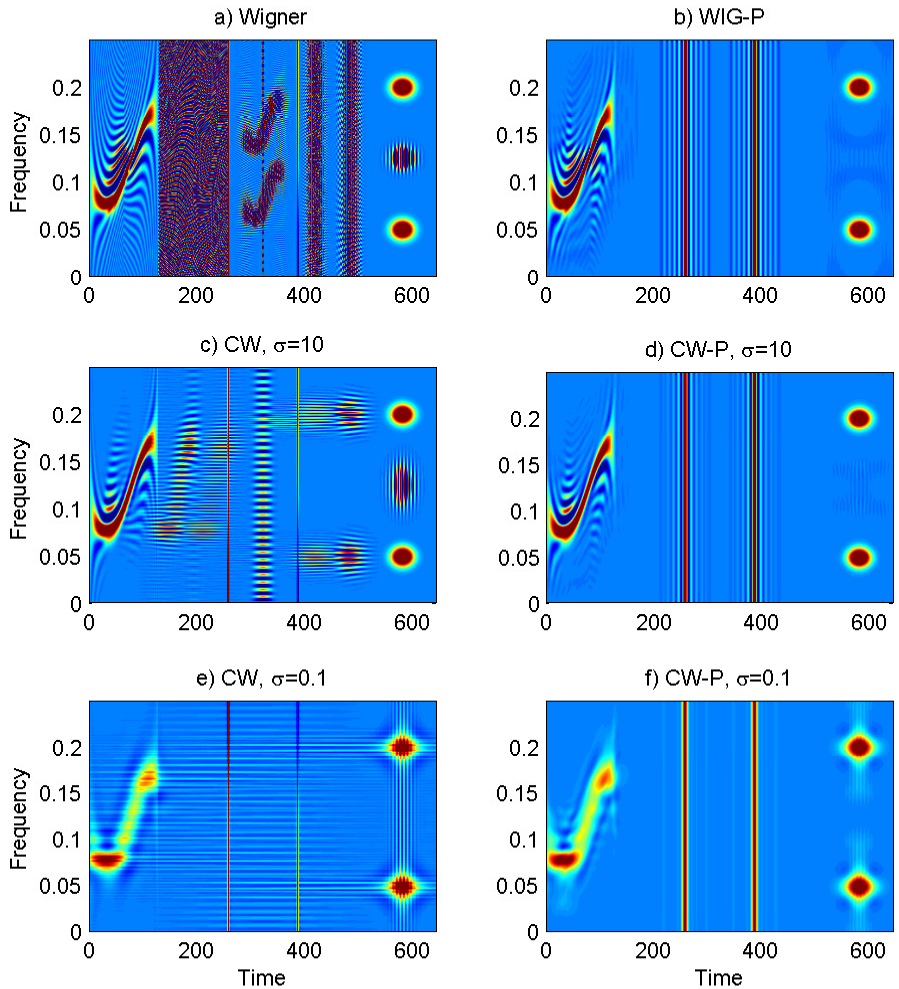

Maria Hansson-Sandsten,'Multitaper Wigner and Choi-Williams distributions with predetermined Doppler-lag bandwidth and sidelobe suppression, Signal Processing, 2011.

Concentration measures

Many of the proposed methods in time-frequency analysis are devoted to suppression of cross-terms and to maintain the concentration of the autoterms. To measure this and possibly automatically determine parameters, measurement criteria for the concentration are needed.

Probability theory example

We use N non-negative numbers, $p_1,\ p_2,\ \ldots,\ p_N$ where $p_1 + p_2 + \ldots + p_N = 1$. A quadratic test function

$$\gamma = p_1^2 + p_2^2 + \ldots p_N^2,$$

will attend its minimum value when $p_1 = p_2 = \ldots = p_N = 1/N$ (maximally spread) and the maximum value when only one $p_i = 1$ and all the others are zero (minimum spread). Incorporating the unity sum constraint gives final the test function,

$$\gamma = \frac{p_1^2 + p_2^2 + \ldots p_N^2}{(p_1 + p_2 + \ldots + p_N)^2}.$$

The kurtosis measure

For any time-frequency distribution a measure for the time-frequency concentration could be defined as,

$$\gamma = \frac{\int_{-\infty}^{\infty}\int_{-\infty}^{\infty} W^4(t,f)dt\,df}{(\int_{-\infty}^{\infty}\int_{-\infty}^{\infty} W^2(t,f)dt\,df)^2},$$

which is similar to the often used **kurtosis** in statistics. For a well concentrated distribution, γ will be large.

Rényi entropy

Another measure is based on what is called the **Rényi entropy** and defined as

$$R_\alpha = \frac{1}{1-\alpha} \log_2\left(\int_{-\infty}^{\infty}\int_{-\infty}^{\infty} W^\alpha(t,f)dtdf\right), \quad \alpha > 0,$$

where $W(t,f)$ is normalized to unity energy. In time-frequency analysis $\alpha = 3$ is commonly used today. We can note that for $\alpha \to 1$ we find the **Shannon entropy**, known from information theory.

Matched Gaussian Multitaper spectrogram

For oscillating Gaussian signal

$$z(t) = g(t - t_0)e^{-i\omega_0 t},$$

the Wigner distribution can be calculated as

$$W_z(t,f) = \sum_{k=1}^{K} \alpha_k S_z^{h_k}(t,f),$$

where $S_z^{h_k}(t,f)$ is the spectrogram from the k:th Hermite function and $K \to \infty$. The weights are shown to be $\alpha_m = 2$ and $\alpha_{m+1} = -2$ for $m = 2k - 1$.

Maria Hansson-Sandsten, 'Matched Gaussian Multitaper Spectrogram', EUSIPCO, Marrakech, Morocko, 2013.

Matched Gaussian Multitaper spectrogram

We minimize

$$e_{min} = \min_{\alpha_k} \int_t \int_\omega \left(\sum_{k=1}^{K} \alpha_k S_g^{h_k}(t,\omega) - W_g(t,\omega) \right)^2 , \qquad (1)$$

for varying K and a two-component signal.

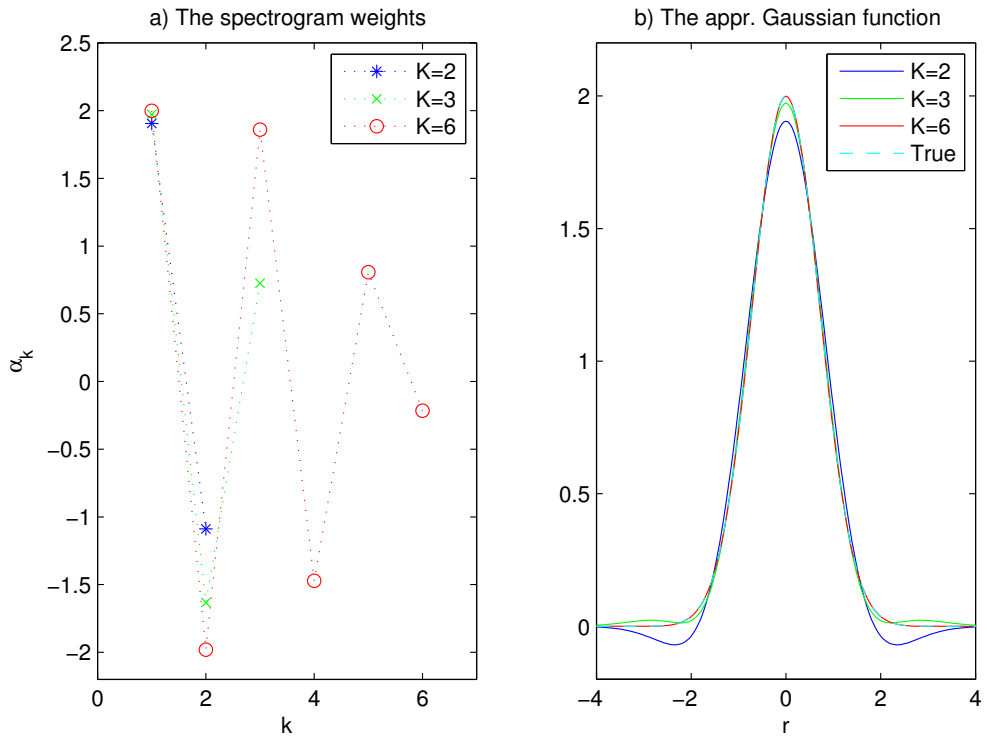

Matched Gaussian Multitaper spectrogram

A measure similar to the statistical kurtosis, which measures the sharpness of a distribution is

$$\mathrm{TFC} = \frac{\sum_{n_0}^{n_1} \sum_{m_0}^{m_1} S^4(n,m)}{(\sum_{n_0}^{n_1} \sum_{m_0}^{m_1} S^2(n,m))^2}.$$

The Gini index organizes the two-dimensional matrix $S(n,m)$ into a sorted vector, $s(1) \leq s(2) \ldots \leq s(N)$, and is defined as

$$\mathrm{GI} = 1 - 2\sum_{l=1}^{N} \frac{s(l)}{||x||_1} \frac{N - l + 0.5}{N},$$

where the l_1-norm is defined $||x||_1 = \sum_{l=1}^{N} |s(l)|$. For both TFC and GI, a higher concentration results in larger values of the measures.

Matched Gaussian Multitaper spectrogram

The Rényi entropy is defined as

$$\mathrm{RE} = \frac{1}{1-\alpha} \log_2 \sum_{n_0}^{n_1} \sum_{m_0}^{m_1} \left(\frac{S(n,m)}{\sum_{n_0}^{n_1} \sum_{m_0}^{m_1} S(n,m)} \right)^{\alpha},$$

with $\alpha = 3$. The Rényi entropy adopt the lowest value for the Wigner distribution of a single Gaussian shaped transient signal, but does not account for the cross-terms. The volume normalized Rényi entropy, takes the cross-terms into account, and is defined as

$$\mathrm{VRE} = \frac{1}{1-\alpha} \log_2 \sum_{n_0}^{n_1} \sum_{m_0}^{m_1} \left(\frac{S(n,m)}{\sum_{n_0}^{n_1} \sum_{m_0}^{m_1} |S(n,m)|} \right)^{\alpha}.$$

For both RE and VRE, a higher concentration of components results in smaller values of the measures.

Matched Gaussian Multitaper spectrogram

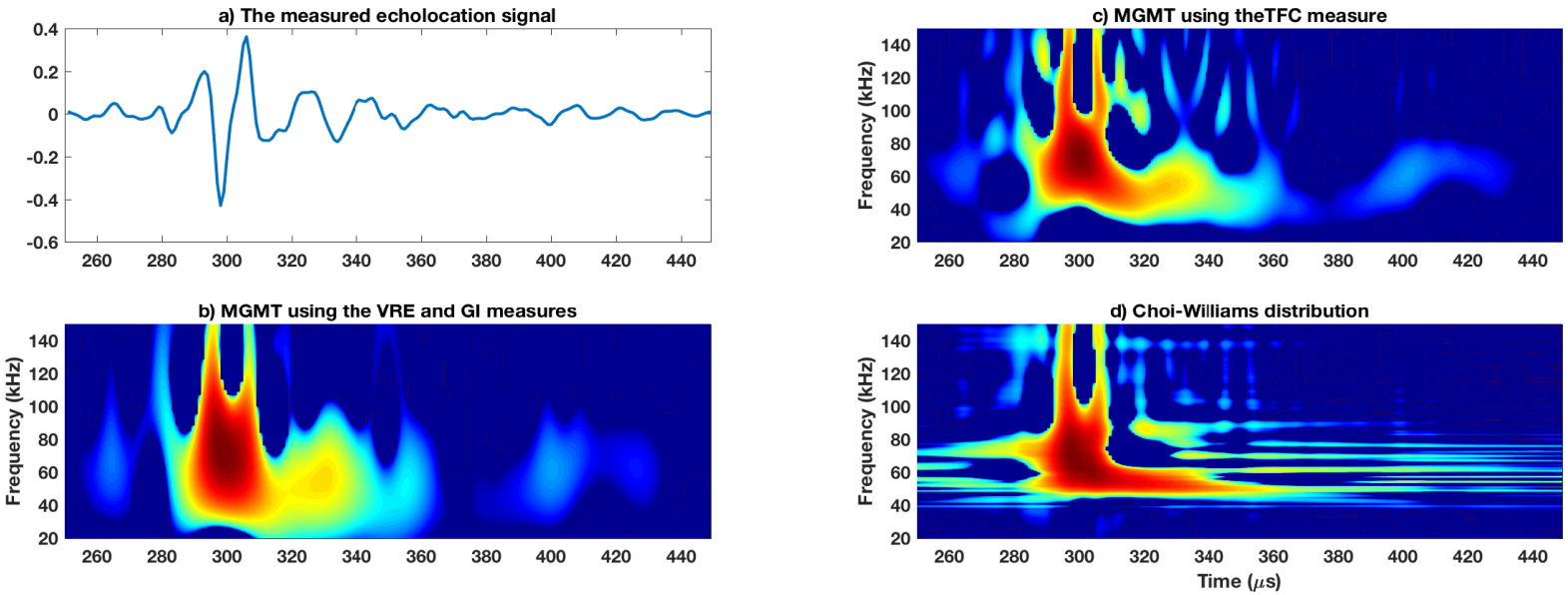

Maria Sandsten, Isabella Reinhold and Josefin Starkhammar, 'Automatic time-frequency analysis of echolocation signals using the matched Gaussian multitaper spectrogram', INTERSPEECH 2017.